DOI: 10.1534/genetics.105.040667

A Screen for Genes Regulating the Wingless Gradient in Drosophila Embryos

Sabrina C. Desbordes,[1] Dhianjali Chandraratna and Bénédicte Sanson[2]

Department of Genetics, University of Cambridge, Cambridge CB2 3EH, United Kingdom

Manuscript received January 10, 2005
Accepted for publication March 10, 2005

ABSTRACT

During the development of the Drosophila embryonic epidermis, the secreted Wingless protein initially spreads symmetrically from its source. At later stages, Wingless becomes asymmetrically distributed in a Hedgehog-dependent manner, to control the patterning of the embryonic epidermis. When Wingless is misexpressed in *engrailed* cells in *hedgehog* heterozygous mutant embryos, larvae show a dominant phenotype consisting of patches of naked cuticle in denticle belts. This dose-sensitive phenotype is a direct consequence of a change in Wg protein distribution. We used this phenotype to carry out a screen for identifying genes regulating Wingless distribution or transport in the embryonic epidermis. Using a third chromosome deficiency collection, we found several genomic regions that showed a dominant interaction. After using a secondary screen to test for mutants and smaller deficiencies, we identified three interacting genes: *dally*, *notum*, and *brahma*. We confirmed that *dally*, as well as its homolog *dally-like*, and *notum* affect Wingless distribution in the embryonic epidermis, directly or indirectly. Thus, our assay can be used effectively to screen for genes regulating Wingless distribution or transport.

SECRETED signaling molecules play an essential role in patterning developing metazoans. Work from recent years shows that the signaling activity of these molecules is tightly regulated (Freeman 2000). Among various levels of regulation, controlling the distribution of ligands in a field of cells is necessary to establish stable gradients that robustly pattern developing tissues (Vincent and Dubois 2002). The distribution of ligands could conceivably be influenced by many factors, including the concentration of receptors, the composition of the extracellular matrix, or the rate of recycling and degradation of the ligand following internalization. The best-documented case is the regulation of ligand distribution by receptors. For example, in Drosophila, Hedgehog (Hh) range of action is regulated by its receptor Patched: if the Hh-binding domain of Patched is mutated, the spread of Hh is extended in the wing imaginal disc (Chen and Struhl 1996). Another case is the morphogen Decapentaplegic, whose concentration gradient is regulated by the amount of its receptor Thickveins (Lecuit and Cohen 1998; Tanimoto *et al.* 2000). In addition to canonical receptors, low-affinity receptors such as heparan sulfate proteoglycans are likely to affect ligand distribution. For instance, in wing discs, mutants that impede the synthesis of heparan sulfate change Hh distribution (Bellaiche *et al.* 1998; The *et al.* 1999; Takei *et al.* 2003; Han *et al.* 2004a,b).

Gradient formation also depends upon the mechanism by which signaling ligands move in the plane of epithelia. It is not yet clear what these mechanisms are, but two main modes of transport have been proposed (reviewed by Vincent and Dubois 2002; Gonzalez-Gaitan 2003): (1) facilitated diffusion, where ligands diffuse within the extracellular space, and this diffusion is modulated by cell-surface receptors, and (2) transcytosis, where ligands are transported along the plane of the epithelium by repeated cycles of endocytosis and recycling to the cell surface.

In this study, we searched for genes that influence the distribution or transport of the signaling ligand Wingless (Wg), the homolog of vertebrate Wnt-1 in Drosophila. In the embryonic epidermis, Wg acts at a short range to regulate the activity of target genes, whereas it behaves as a long-range morphogen in the wing imaginal disc (reviewed by Seto and Bellen 2004). In the wing, Wg forms a stable gradient with a source localized at the boundary between ventral and dorsal compartments and triggers the expression of target genes at different distances from its source in a concentration-dependent manner (Zecca *et al.* 1996; Neumann and Cohen 1997).

Both facilitated diffusion and transcytosis have been proposed to explain how Wg moves from cell to cell. In the embryonic and imaginal disc epithelia, Wg protein is detected in the basolateral extracellular space as well as in bright intracellular dots localized to the apical side of the cells (Pfeiffer *et al.* 2000; Strigini and Cohen 2000; Greco *et al.* 2001; Simmonds *et al.* 2001). These

[1]*Present address:* Laboratory of Stem Cell and Tumor Biology, Neurosurgery and Developmental Biology, Memorial Sloan Kettering Cancer Center, 1275 York Ave., New York, NY 10021.

[2]*Corresponding author:* Department of Genetics, University of Cambridge, Downing St., Cambridge CB2 3EH, United Kingdom. E-mail: bs251@mole.bio.cam.ac.uk

punctate structures are thought to coincide with both exocytic and endocytic vesicles (van den Heuvel *et al.* 1989; Gonzalez *et al.* 1991; Pfeiffer *et al.* 2000, 2002), and have been proposed to be involved in the transport of Wg from cell to cell in embryos (transcytosis model) (Bejsovec and Wieschaus 1995; Moline *et al.* 1999). In the wing, some of these structures colocalize with vesicles termed argosomes, which have also been suggested to move from one cell to the next through the endocytic compartment (Greco *et al.* 2001). On the other hand, other studies have proposed that these vesicles represent Wg secretion rather than Wg movement (Pfeiffer *et al.* 2000; Strigini and Cohen 2000). A second model proposed for Wg transport is diffusion through the extracellular space. In support of this model, Strigini and Cohen (2000) found that most of the Wg gradient is extracellular in the wing disc and that the speed of Wg movement is compatible with diffusion within the extracellular space. Wg tightly associates with the cell surface (Reichsman *et al.* 1996), so it is unlikely to diffuse freely, but it could spread through facilitated diffusion by interacting with cell surface receptors. Consistent with this, one of the factors that influences the shape of the Wg gradient in the wing disc is the receptor Frizzled2 (Fz2) (Cadigan *et al.* 1998). When Fz2 is overexpressed, Wg appears to be stabilized at the cell surface. The amount of detectable Wg protein increases and this correlates with a broadening of Wg-signaling range. Recently, another factor found to affect the shape of the Wg gradient in wing discs is Notum, a hydrolase that is thought to modify the heparan sulfate chains of the glypicans Dally and Dally-like (Gerlitz and Basler 2002; Giraldez *et al.* 2002). When Notum is overexpressed in the disc, the spread of Wg is reduced (Giraldez *et al.* 2002). Apart from transcytosis and facilitated diffusion, a third mode of transport for Wg has been documented in the embryonic epidermis: cells expressing Wg are able to move away from the source while transporting active Wg protein in secretory vesicles (Pfeiffer *et al.* 2000).

Here we focus our analysis of Wg distribution and transport to the embryonic epidermis. An interesting aspect of the embryonic Wg gradient is that it becomes asymmetric early in embryogenesis (Gonzalez *et al.* 1991). In the abdomen, *Wg* is expressed in a single row of cells in each embryonic segment, immediately anterior to two to three rows of cells expressing *engrailed* (*en*) and *hh* (Figure 1A). *Wg*, *en*, and *hh* maintain each other's expression initially and then act as a bipartite organizer to control intrasegmental patterning (reviewed in Hatini and DiNardo 2001; Sanson 2001). Early on (at stage 9/10), Wg spreads symmetrically from its source over a few cell diameters. This stage coincides with the time when *en* expression in the adjacent cells requires Wg signaling for its maintenance. Later on (from stage 11 onward), the Wg gradient becomes asymmetric (Figure 1A). Wg is undetectable posterior to the *wg*-expressing cells, except occasionally in some cells immediately adjacent to the source (Sanson *et al.* 1999). By contrast, Wg is detectable over a few cell diameters in the anterior direction. This asymmetric distribution of Wg protein translates into an asymmetric range in Wg signaling. At midembryogenesis, Wg signaling represses the expression of *shavenbaby*, a gene required for denticle formation in the embryonic epidermis (Payre *et al.* 1999). Thus, the secretion of smooth or naked cuticle provides a convenient readout of Wg-signaling activity (Lawrence *et al.* 1996). Matching the asymmetric distribution of Wg protein, naked cuticle is secreted four to five cell diameters anterior to the Wg source, but only one cell diameter posterior to it, which corresponds to the anterior-most row of Engrailed-expressing cells (Dougan and DiNardo 1992; O'Keefe *et al.* 1997; Sanson *et al.* 1999) (Figure 1A).

One mechanism that contributes to the asymmetric shape of the Wg gradient is the clearing of the receptors Fz and Fz2 from the En domain through downregulation of their transcription (Lecourtois *et al.* 2001). Presumably, the decrease in the concentration of Fz and Fz2 destabilizes Wg, perhaps by making it accessible to proteases (Cadigan *et al.* 1998). However, although this is enough to restrict Wg range initially, an additional mechanism, which involves accelerated degradation of Wg protein posterior to the Wg source, is required later on (Dubois *et al.* 2001). Epidermal growth factor receptor signaling is required for this increase in Wg turnover, although the molecular mechanism is not known (Dubois *et al.* 2001).

In terms of genetic regulation, Hh, which is secreted by the En cells, is the top regulator in making the embryonic Wg gradient asymmetric (Sanson *et al.* 1999). This was shown by expressing *wg* in the En domain—using the UAS/Gal4 system—in a *hh* mutant background. In *enGal4/UASwg [hh$^-$/hh$^-$]* embryos, the expression of *en* and *wg* is maintained because of the artificial regulatory loop between the two genes, which bypasses the need for Hh signaling. In *enGal4/UASwg* embryos, row 1 of each denticle belt is missing but the shape of the gradient remains asymmetric (Figure 1B). By contrast, in *enGal4/UASwg [hh$^-$/hh$^-$]* embryos, Wg is detected in a symmetric gradient, with Wg spreading posterior as well as anterior to the source (Sanson *et al.* 1999) (Figure 1C). This is reflected in the cuticle pattern: naked cuticle is secreted four to five cell diameters on both sides of the source (Figure 1C). The same phenotype is seen when *cubitus interruptus*, a downstream component of the Hh pathway, is removed in *enGal4/UASwg* embryos (Sanson *et al.* 1999). This shows that Hh signaling controls the expression of one or several genes that regulate Wg distribution.

The requirement for Hh signaling is dose sensitive: when one copy (instead of two) of Hh is removed in *enGal4/UASwg* embryos, patches of naked cuticle are found within denticle belts (Figure 1D). We used this

dominant phenotype in a F_1 screen to find genes giving a similar phenotype, and thus potentially regulating Wg distribution. We conducted a deficiency screen on the third chromosome to identify such genes. Two successive screens led us to the identification of three genes that affect Wg distribution in the embryonic epidermis: *dally, dally-like*, and *notum*. An additional role for *dally-like* in Hh signaling, found while analyzing these results, has been described elsewhere (Desbordes and Sanson 2003).

MATERIALS AND METHODS

Fly stocks: The Bloomington Drosophila Stock Center (BDSC) provided the third chromosome deficiency kit (see list of stocks in the appendix) as well as *Df(3L)Scf-R11, Df(3R)l26c, Df(3R)ry75, Df(3R)urd*, and *Df(3R)lc4a*. The Umea Stock Center (USC) provided *Df(3L)th102*; Ken Cadigan, *Df(3L)Dfz2*; Daniel Kalderon, *Df(3L)A27*; and Daniel St Johnston, *Df(3L)XS-543*. We obtained the following mutant stocks from the BDSC: *l(3)06464*, *l(3)01629*, arf^{72A}, brm^{2}, pip^{1}, kni^{10}, Dl^{3}, and hh^{AC}. $Dfz2^{C1}$ was provided by Gary Struhl, $dally^{10}$ and $dally^{E385}$ by Steve Kerridge, Psn^{B3} and Psn^{C4} by Mark Fortini, pip^{2} and kni^{8} by USC, brm^{T362} and brm^{T485} by Jessica Treisman, and not^{3} and not^{5} by Steve Cohen.

The transgenic strains used were *enGal4* (Andrea Brand, University of Cambridge, UK), *UASwg* (Lawrence *et al.* 1996), and *UASGFP* (Nick Brown, University of Cambridge, UK). We combined these lines to generate the following genotypes: *w; enGal4/+; UASwg/+* (abbreviated as *enGal4/UASwg*); *w; enGal4/+; UASwg.*hh^{AC}/hh^{AC} (abbreviated as *enGal4/UASwg*[hh^{-}/hh^{-}]); and *w; enGal4/+; UASwg.*hh^{AC}/+ (abbreviated as *enGal4/UASwg*[hh^{-}/+]).

To generate germline clones, we used the stocks *y w hsflp; Dr/TM3* (BDSC), *w; FRT80B* ovo^{D1}/*TM3Sb* (from D. St Johnston), and *w; FRT80B* not^{3}/*TM6B* (from S. Cohen). *y w hsflp; ; FRT80B* ovo^{D1}/ *FRT80B* not^{3} larvae were heat-shocked 1 hr at 37° between 72 and 96 hr of development, and another heat shock was performed 24 hr later. The females derived from these larvae were crossed with either *w; FRT80B* not^{3}/*TM3actin-GFP* males to analyze the cuticle of the embryos or *w; enGal4. UASGFP; FRT80B* not^{3}/*TM3hunchback-lacZ* males to analyze embryos by immunostainings. The marked balancers *TM3actin-GFP* (*TM3GFP*) and *TM3hunchback-lacZ* (*TM3LacZ*) were supplied by the BDSC.

Screening procedure: Each deficiency stock from the third chromosome kit was crossed to the *enGal4* stock to generate *engal4/+; deficiency/+* F_1 males. We used dominant markers present on the balancer chromosome in the deficiency stock to identify unambiguously the F_1 males carrying the deficiency (in several cases we had to rebalance the stock or use different dominant markers to facilitate the identification). For a few deficiencies from the kit, the F_1 *engal4/+; deficiency/+* males did not survive or were sterile. About 50 *UASwg* virgins were then crossed to 10–30 F_1 *engal4/+; deficiency/+* males (see scheme in Figure 2A), and embryos were collected overnight at 25° on grape juice agar plates. The temperature was controlled carefully since the UAS/Gal4 system is sensitive to temperature. Note that we had to use F_1 *engal4/+; deficiency/+* males instead of F_1 *engal4/+; deficiency/+* females in the screen, because the *enGal4; UASwg* embryos derived from *engal4/+* females were deformed and presented many gaps of naked cuticle in the denticle belts. The reason for this phenotype is unclear (*enGal4* might be weakly expressed maternally), but it made it impossible to consistently score additional gaps from interacting deficiencies.

Since *enGal4/UASwg* embryos die at the end of embryogenesis, the collected embryos were aged at least 30 hr so that only nonviable embryos remain unhatched. Dead embryos were dechorionated using bleach and their vitelline membrane was removed by hand in Hoyer's on a slide. Embryos were aligned ventral side up in a mixture of Hoyer's and lactic acid (1:1). Cuticle preparations were baked overnight at 55°.

Gaps were scored by visualizing the cuticles with phase-contrast microscopy. For abdominal belts A2–A7, we scored a gap when a patch of smooth cuticle replaced most rows of denticles in the belt (Figure 2, D *vs.* D′). Because A1 is thinner than the other abdominal denticle belts, we scored only complete breaches of this belt (Figure 2, E *vs.* E′). We eliminated segment A8 from our analysis, because it was too often folded and difficult to visualize.

To assess the significance of our results, we compared the number of gaps obtained for each deficiency with the number of gaps obtained for wild-type chromosomes. We scored five gaps for 354 *enGal4/UASwg* embryos examined, when chromosomes from the wild-type yw^{67} or $canton^{S}$ strains were tested in place of a deficiency chromosome in the screening scheme (Table 1). We used this value as the expected frequency of gaps and employed a standard χ^2 test to compare this expected frequency with the frequency of gaps observed for each deficiency. When the *P*-value was <0.05, a deficiency was considered not interacting (appendix).

RNA interference: The technique of RNA interference (RNAi) was carried out following the protocol described in Desbordes and Sanson (2003). Briefly, ~300-nucleotide-long sequences from the plasmids pBS(KS)-*dlp* (Baeg *et al.* 2001) and pBS(KS)-*dally* (Nakato *et al.* 1995) were amplified using primers pairs containing a T7 promoter sequence (5′-TAA TACGACTCACTATAGG-3′) at the 5′-end. The PCR products were used as templates for T7 transcription reactions with the Ribomax large-scale RNA production kit (Roche). Following phenol/chloroform extraction and ethanol precipitation, the double-stranded RNA (dsRNA) was resuspended in Spradling injection buffer and injected at a concentration of ~8 μg/μl in blastoderm embryos.

***In situ* hybridizations of whole-mount embryos:** Embryos were fixed and hybridized with a digoxygenin single-stranded RNA probe as described by (Jowett 1997), except that no proteinase K treatment was performed. The *wingless* cDNA was a gift from J. P. Vincent.

Antibody stainings: Immunofluorescence was performed on fixed embryos according to standard protocols. Primary antibodies used were mouse anti-Wingless 4D4 (1:10) (from the Developmental Studies Hybridoma Bank) and rabbit anti-GFP (1:300) (Abcam). Secondary antibodies were Alexa fluorescent conjugates from Molecular Probes (Eugene, OR; Alexa 488 and Alexa 594). The GFP antibody staining was used to label Engrailed-expressing cells in embryos carrying the *enGal4.UASGFP* transgene combination (see Figure 5, E–E″, and Figure 6, C–D′). To visualize the Wg gradient, five to seven confocal sections were collected every 0.3 μm, starting from the apical surface of the cells, and projected. Sections were collected on a Bio-Rad (Richmond, CA) MRC1024 confocal microscope.

RESULTS

Screen design: In stage 12 wild-type or *enGal4/UASwg* embryos, the Wg gradient is asymmetric, and as a consequence, naked or smooth cuticle is secreted anterior to the Wg source, whereas a belt of denticles is secreted

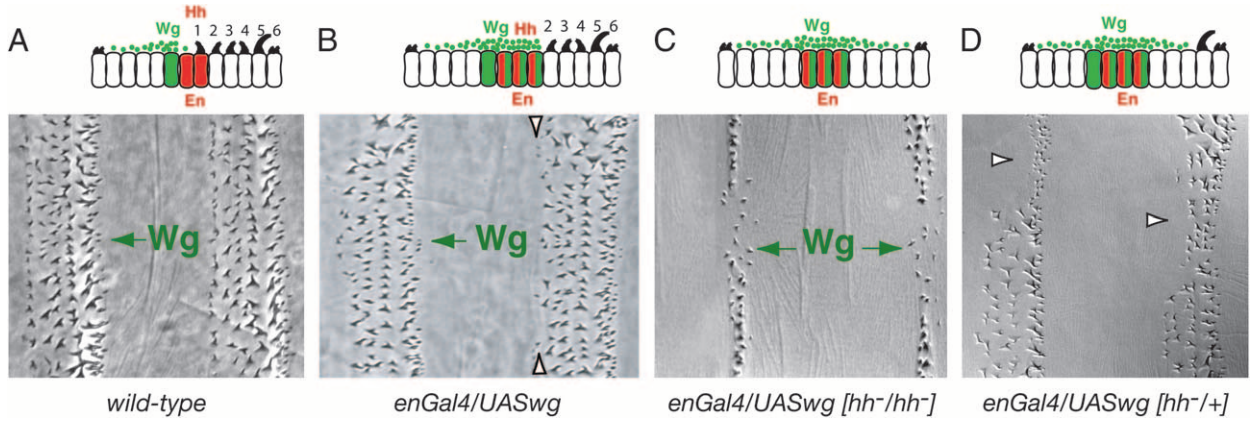

FIGURE 1.—Shape of the Wingless embryonic gradient in different genetic contexts. The diagrams depict the distribution of Wg protein at stage 12 in different genetic contexts. For clarity, Wingless protein distribution has been drawn above the cells, but in the epithelium the Wingless protein is detected both in the extracellular space and in bright intracellular dots, which are mostly apical (see Introduction). On the same diagrams the type of cuticle secreted by each cell at the end of embryogenesis is represented. The corresponding cuticle pattern is shown below. (A) In wild-type embryos, the Wg gradient is asymmetric after stage 11. Wg is expressed in one row of cells in each segment (green cell in diagram). At stage 12, Wg protein can be detected up to four to five cells anterior to the Wg source, but only occasionally in the first row of En cells (in red). As a consequence of this asymmetric gradient, naked cuticle is later on secreted up to four to five cell diameters anterior to the Wg source, but only in the adjoining En cells in the posterior direction. At the time of cuticle deposition (from stage 15 onward), the En stripe is, on average, two cells wide, with the second cell row secreting the first row of each denticle belt in abdominal segments A2–A7. In these segments, each belt is made of six rows of cells making denticles. (B) When Wg is expressed in the En cells, the gradient remains asymmetric. More En cells are specified, and they express a high level of Wg protein. As a consequence, row 1, which should be specified by the posterior-most En cell, disappears completely or partially in all abdominal denticle belts (arrowheads). However, immediately posterior to the En domain, the denticle rows are specified normally, and no Wg protein can be detected there. (C) Expressing Wg in the En cells allows us to remove *hh* without losing En expression. This reveals the role of Hh in making the Wg gradient asymmetric: in *enGal4/UASwg[hh⁻/hh⁻]* embryos, Wg protein is detected posterior as well as anterior to the En domain, and the gradient is symmetric in shape. Consequently, naked cuticle is made over four to five cell diameters posterior as well as anterior to the En domain. Instead of denticle belts, a thin stripe of denticles similar to row 6 denticles is secreted. (D) An intermediate phenotype is seen in *enGal4/UASwg[hh⁻/+]* embryos: small regions of naked cuticle are found within denticle belts, often replacing denticle rows 2–5 (arrowheads).

posterior to it in each abdominal segment at the end of embryogenesis (Figure 1, A and B; see also Figure 4, A and B). The only difference between the cuticle phenotype of wild-type and *enGal4/UASwg* embryos is the loss of the first row of denticles in the latter embryos. The patches of naked cuticle found within the denticle belts of *enGal4/UASwg [hh⁻/+]* embryos correspond to regions of the epithelium where Wg diffuses symmetrically (Figure 1D) (SANSON *et al.* 1999). We call these patches "gaps" and refer to the dominant phenotype as a "gap" phenotype. We reasoned that genes controlling the shape of the Wg gradient downstream of Hh signaling should exhibit a similar dominant phenotype. On the basis of this hypothesis, we screened the Bloomington collection of large deficiencies on the third chromosome for those that give a gap phenotype in the *enGal4/UASwg* background. As a control, we also tested in this sensitized background two wild-type chromosomes (yw^{67} and $canton^{S}$) and three different *hh* mutations: a hypomorph (hh^{5}), a null allele (hh^{AC}), and a deficiency removing the *hh* locus (*Df(3R)hh*).

The crossing scheme for the screen is given in Figure 2A. First, *enGal4* flies were crossed with flies carrying the chromosome to be tested. Then F_1 males carrying one copy of *enGal4* and one copy of a deficiency chromosome (or a wild-type or mutant chromosome) were crossed with *UASwg* females to generate *enGal4/UASwg [deficiency/+]* embryos. The genotype *enGal4/UASwg* is embryonic lethal (the embryos do not hatch due to a deformed head) and we therefore collected all the dead embryos from this cross for cuticle analysis. Dead *enGal4/UASwg* embryos are easily distinguished from the occasional dead wild-type embryos by the fact that row 1 is missing from abdominal denticle belt A2–A7 (Figure 2, C *vs.* D). In this crossing scheme, half of the *enGal4/UASwg* embryos are heterozygous for a deficiency chromosome (or a wild-type or mutant chromosome), while the other half is wild type (Figure 2A).

We then scored the number of *enGal4/UASwg* embryos that showed patches of naked cuticle in the abdominal denticle belts A1–A7 (Figure 2, D′ and E′), using strict criteria (see MATERIALS AND METHODS). We found a very low frequency of gaps when we tested wild-type chromosomes in our screen: yw^{67} gave 1.9% of embryos with gaps ($n = 106$) and $canton^{S}$, 1.2% ($n = 248$) (Table 1). This gives an average of 1.4% of embryos with gaps ($n = 354$) for the wild-type control. By contrast, all *hh* alleles tested gave a high proportion of

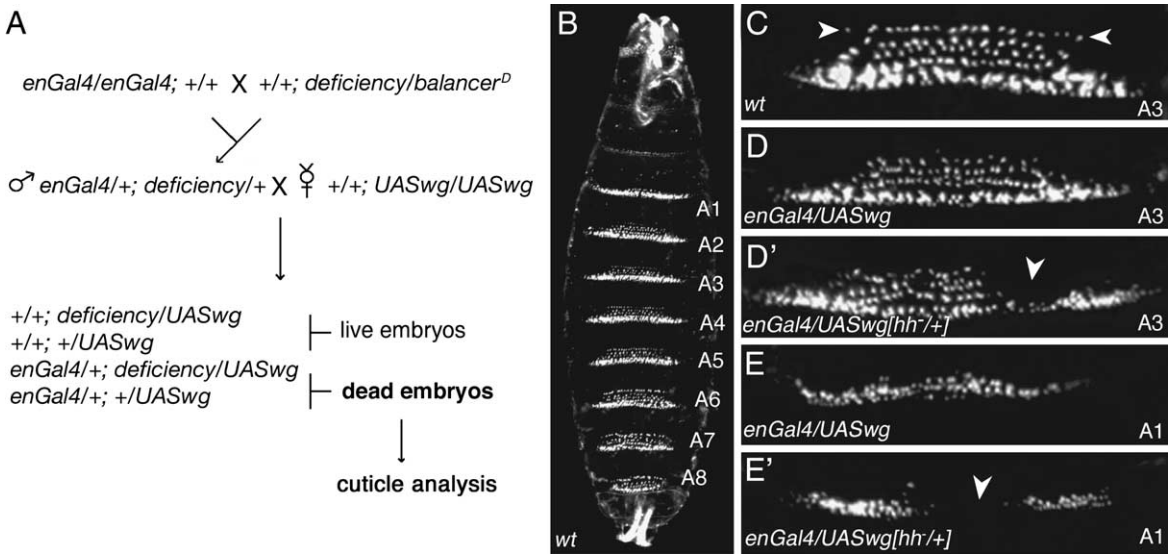

FIGURE 2.—Screen for dominant phenotypes in the *enGal4/UASwg*-sensitized background. (A) To produce *enGal4/UASwg* embryos heterozygous for a given deficiency chromosome, two successive crosses were performed: first, *enGal4* flies were crossed to flies carrying a deficiency over a balancer chromosome with a dominant visible mutation. In the next cross, F_1 males that do not exhibit the dominant visible mutation, and therefore are heterozygous for *enGal4* and the deficiency chromosome, were selected and crossed to virgin *UASwg* females. Half of the progeny from this cross do not hatch at the end of embryogenesis: these are the embryos carrying *enGal4/UASwg*, which have a deformed head and cannot get out of the egg shell. All the dead embryos are collected and mounted ventral side up for cuticle analysis. (B) Ventral side of wild-type larvae just after hatching (head is up). The eight abdominal segments are indicated. Row 1 is clearly seen in A2–A8. (C) Close-up of denticle belt in wild-type A3 segment. Row 1 is indicated by arrowheads. (D) Close-up of denticle belt in the A3 segment of *enGal4/UASwg* embryos. Row 1 is clearly missing, which allows us to distinguish unambiguously the dead embryos of the *enGal4/UASwg* genotype from occasional wild-type dead embryos. (D′) Dominant phenotype found in *enGal4/UASwg[hh⁻/+]* embryos. A region of ectopic naked cuticle is shown in the denticle belt of segment A3 (arrowhead). We score this phenotype as a gap in the screen. (E) The denticle belt in segment A1 is thinner than that in other abdominal segments. (E′) For segment A1, we scored a gap when the belt was completely breached by ectopic naked cuticle, as shown here in a *enGal4/UASwg[hh⁻/+]* embryo (arrowhead).

embryos exhibiting gaps in the denticle belts: 20% (n = 130) for hh^5, 28.2% (n = 174) for hh^{AC}, and 36.5% (n = 138) for *Df(3R)hh* (Table 1). As expected, the hypomorphic allele, hh^5, gives a lower proportion of embryos with the dominant phenotype compared to the stronger mutant hh^{AC} and the deficiency *Df(3R)hh*. Since only half of the *enGal4/UASwg* embryos scored with our scheme are actually heterozygous for the *hh* mutations tested (Figure 2A), these results mean that ~60% of embryos of the *enGal4/UASwg [hh⁻/+]* genotype exhibit a dominant phenotype.

Primary screen: We then screened the collection of deficiencies on the third chromosome for those that showed the dominant phenotype at a frequency significantly higher than that of the wild-type control. We scored gaps in *enGal4/UASwg* embryos derived from males heterozygous for a given deficiency and used a χ^2 test to assess the significance of our results (see MATERIALS AND METHODS). A total of 59 of the tested deficiencies did not show a frequency of embryos with gaps significantly different from the wild type ($P > 0.05$). For these deficiencies, the percentage of embryos exhibiting the dominant phenotype varies from 0 to 3.3% (APPENDIX). Seven deficiencies interacted weakly in the screen ($0.001 < P < 0.05$), with percentages of embryos with gaps varying from 4.1 to 7.1% (APPENDIX). These are deficiencies *Df(3L)h-i22*, *Df(3L)Scf-R6*, *Df(3L)brm11*, *Df(3L)VW3*, *Df(3L)rdgC-co2*, *Df(3R)ry615*, and *Df(3R)Dl-BX12*, shown in red in Figure 3. Two deficiencies,

TABLE 1

Testing wild-type and *hedgehog* mutant chromosomes in the screen

Chromosome tested	Total no. of *enGal4/UASwg* embryos	No. of *enGal4/UASwg* embryos with gaps
yw^{67}	106	2 (1.9%)
$canton^S$	248	3 (1.2%)
Average wild type	354	5 (1.4%)
hh^5	130	26 (20%)
hh^{AC}	174	49 (28.2%)
Df(3R)hh	138	50 (36.5%)

Chromosomes from two different wild-type strains, yw^{67} and $canton^S$, were tested in the screen. In both cases, the number of *enGal4/UASwg* embryos presenting ectopic naked cuticle posterior to the Wg source (gaps) was very low. By contrast, each mutant allele of *hh* tested gave a high proportion of gaps in the *enGal4/UASwg* background. Numbers in parentheses are percentages.

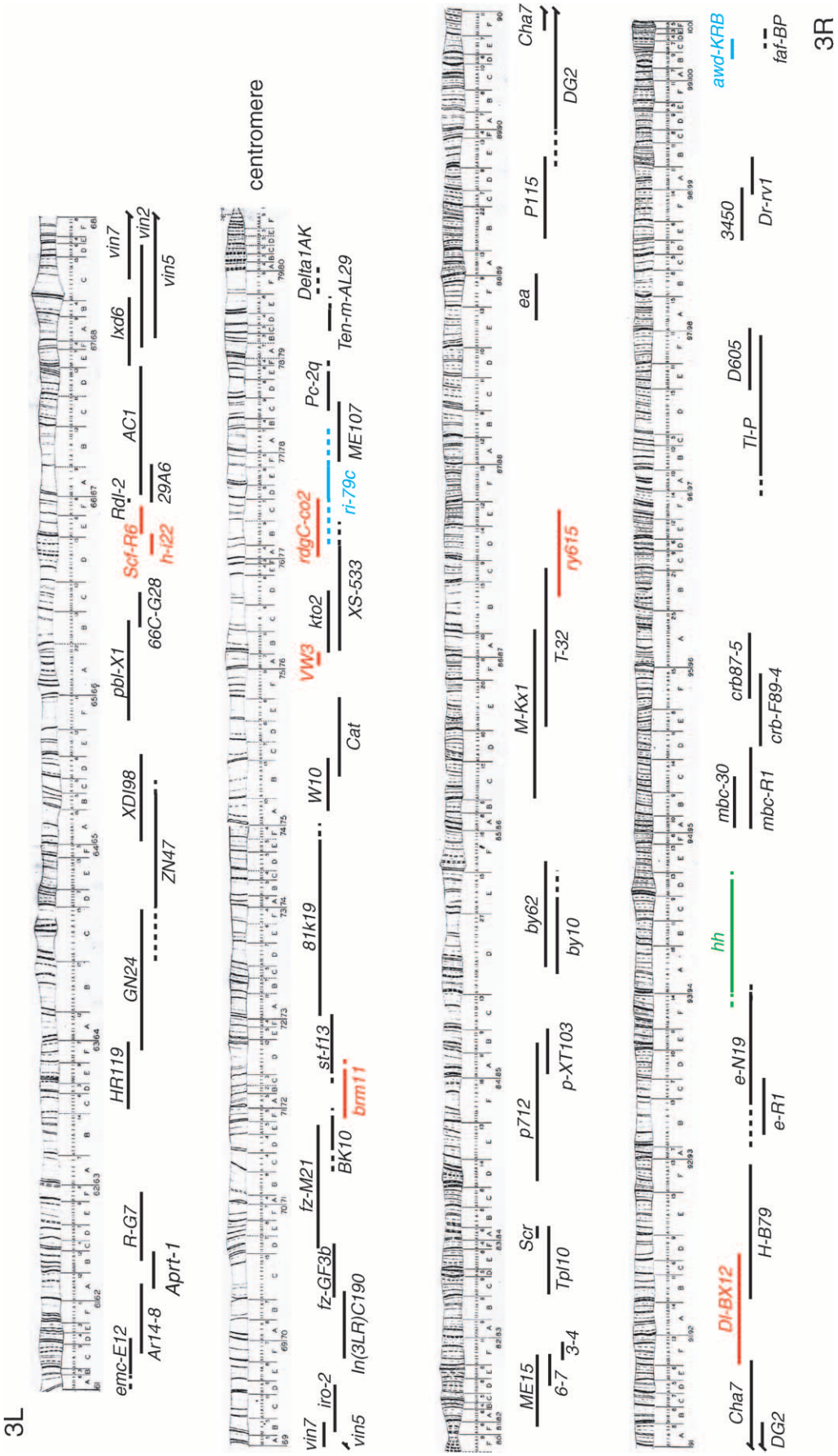

FIGURE 3.—Map of the deficiencies on chromosome 3 tested in the primary screen. Deficiencies from the Bloomington deficiency kit are positioned on a drawing of polytene chromosome 3 (adapted from LINDSLEY and ZIMM 1992) according to cytological positions given in FlyBase (http://flybase.bio.indiana.edu/). Cytological positions are indicated under the drawing. 3L and 3R indicate left arm and right arm of chromosome 3, respectively. Deficiencies that did not interact are indicated in black. The deficiency that uncovered the *hh* locus is shown in green. Deficiencies that interacted strongly ($P < 0.001$) are shown in blue and those that interacted weakly ($0.001 < P < 0.05$) are shown in red.

Df(3L)ri-79c and *Df(3R)awd-KRB*, exhibited a frequency of embryos with gaps close to the frequency observed in *enGal4/UASwg* embryos derived from males hh^{-}/+ (34.2 and 36%, respectively; see APPENDIX). These deficiencies are shown in blue in Figure 3.

For *Df(3L)ri-79c* and *Df(3R)awd-KRB*, we tested the possibility that the dominant phenotype was independent of the *enGal4/UASwg* background. Of the *enGal4/UASwg* embryos, 34.2% ($n = 111$) derived from *Df(3L)ri-79c*/+ males exhibited gaps in the denticle belts, mainly in the A4 segment. By crossing *Df(3L)ri-79c*/+ males with the yw^{67} wild-type strain, we found that 25% ($n = 60$) of the progeny have the same dominant phenotype, thus showing that the dominant phenotype arises independently of the *enGal4/UASwg*-sensitized background. Since *Df(3L)ri-79c* removes the gene *knirps* (*kni*), we tested a null mutation in this gene, kni^{8}, and found that 30% of *enGal4/UASwg* embryos derived from kni^{8}/+ males have gaps in segment A4. This shows that the dominant phenotype detected for *Df(3L)ri-79c* is due to *kni*. The excess naked cuticle found in kni^{-}/+ embryos is unlikely to be a consequence of a change in Wg distribution, since *kni* is a gap gene required in the segmentation cascade early in embryogenesis (for a review, see ST JOHNSTON and NUSSLEIN-VOLHARD 1992). Rather, a perturbation of the transcription pattern of the segmentation genes in segment A4 is likely to cause the dominant phenotype. In support of this, a compression of the expression pattern of the pair-rule gene *fushi-tarazu* has been observed in segments A4 and A5 in kni^{-}/+ embryos (CARROLL and SCOTT 1986).

The same was found for Df(3R)awd-KRB: 36% ($n = 136$) of *enGal4/UASwg* embryos derived from *Df(3R)awd-KRB* /+ males exhibit gaps in the denticle belts. Curiously, the gaps are found in alternating segments (not shown) (DESBORDES 2004). This dominant phenotype is also found in *Df(3R)awd-KRB* /+ embryos, showing that it can occur independently of the *enGal4/UASwg* background. The excess cuticle found in *Df(3R)awd-KRB*/+ embryos had also been noted by COX *et al.* (2000), and the molecular basis for this phenotype is unknown. However, because the dominant phenotype is pair-rule, this again suggests an effect on early segmentation rather than on the regulation of Wg distribution.

We therefore decided to concentrate on the six regions defined by the deficiencies interacting weakly in the screen. Although the percentage of embryos with gaps found for these deficiencies is low (4.1–7.1%), the statistical test indicates that the interactions detected have a reasonable chance to be significant ($0.001 < P < 0.05$). Also, only half of the *enGal4/UASwg* embryos collected in a sample are actually heterozygous for the deficiency tested (the other half are of genotype *enGal4/+; UASwg/+*; see Figure 2A). This means that the true percentage of embryos of genotype *enGal4/+; UASwg/deficiency* showing the dominant phenotype is ~8–14% for these deficiencies, which is significantly higher than the proportion of embryos with gaps found for the genotype *enGal4/+; UASwg/+* (1.4%) (Table 1). We thus performed a secondary screen by testing smaller deficiencies and point mutations that map to these six regions. Table 2 summarizes the findings from the secondary screen, and the details about levels of interaction and cytological positions are given in the APPENDIX.

Secondary screen: *Region 66:* From the primary screen, two interacting deficiencies overlapped in cytological location 66E: *Df(3L)h-i22* (cytological breakpoints 66D10-11 and 66E1-2) and *Df(3L)Scf-R6* (66E1-6 and 66F1-6). *EnGal4/UASwg* embryos derived from *Df(3L)h-i22/+* or *Df(3L)Scf-R6/+* males show a dominant gap phenotype with a similar frequency of 6.4% ($n = 249$) and 7.1% ($n = 210$), respectively. This suggests that the same gene is removed by both deficiencies and that the gene should be found in the region of overlap between the two deficiencies. Moreover, *Df(3L)Scf-R11*, a deficiency that overlaps with the proximal end of *Df(3L)Scf-R6*, did not interact, suggesting that the interacting gene is removed by the distal end of *Df(3L)Scf-R6* (Table 2 and APPENDIX). We mapped genetically the overlap between *Df(3L)h-i22* and *Df(3L)Scf-R6* by complementation tests with sequenced *P*-element insertions in the region. *Df(3L)hi22* failed to complement *l(3)10631* (66D14-15), *l(3)01629* (66DE1-2), and *l(3)06464* (66E1-2) but complements *l(3)10534* (66E2-3). *Df(3L)Scf-R6* complemented *l(3)10631*, but failed to complement *l(3)01629*, *l(3)06464*, and *l(3)10534*. This suggests that the region of overlap between *Df(3L)h-i22* and *Df(3L)Scf-R6* falls between *l(3)10631* and *l(3)10534*, which represents an interval of 215 kb on the genome sequence. This interval contains several genes, including *dally*, one of the two Drosophila homologs of glypicans (the other one is *dally-like*; see below). Dally was particularly interesting since it had been implicated in the regulation of Wg signaling (LIN and PERRIMON 1999; TSUDA *et al.* 1999). A RNA probe corresponding to exons 1–6 of *dally* cDNA was generated and hybridized to polytene chromosomes from *Df(3L)h-i22/+* or *Df(3L)Scf-R6/+* larvae. On wild-type chromosomes, the *in situ* hybridization signal maps at cytological location 66E1-3, which corresponds to the cytology given in FlyBase (data not shown) (DESBORDES 2004). No signal was observed on the deficient chromatid of *Df(3L)h-i22/+* polytene chromosomes, demonstrating that most *dally* sequences are missing in this deficiency (data not shown) (DESBORDES 2004). This shows that *Df(3L)h-i22* is an amorph for *dally*, in contrast to a previous report suggesting that *Df(3L)h-i22* was a hypomorph for this gene (TSUDA *et al.* 1999). On *Df(3L)Scf-R6/+* polytene chromosomes, the signal was clearly reduced on the deficient chromatid, suggesting that some of the sequences present between exons 1 and 6 of *dally* are missing in this deficiency (data not shown; see DESBORDES 2004). *Df(3L)Scf-R6* was generated by X-ray irradiation of *Scf1*, which is an inversion (breakpoints 65A12-15; 66F3) (KOPP and DUNCAN 1997).

TABLE 2

Summary of the interactions detected in the secondary screen

Cytological region on chromosome 3	Deficiencies tested in primary screen	Deficiencies tested in secondary screen	Mutations tested in secondary screen	Gene isolated
Region 66	*Df(3L)h-i22* *Df(3L)Scf-R6* *Df(3L)Rdl-2*	*Df(3L)Scf-R11*	*dally*^{10} *dally*^{E385} *l(3)06464(dally*^{P2}*)* *l(3)01629*	*dally*
Region 72	*Df(3L)BK10* *Df(3L)brm11* *Df(3L)st-f13*	*Df(3L)A27* *Df(3L)th102*	*brm*^{2} *brm*^{T362} *brm*^{T485} *arf*^{72A} *not*^{3} *not*^{5}	*brm, not*
Region 75	*Df(3L)Cat* *Df(3L)VW3* *Df(3L)kto2*	*Df(3L)Dfz2*	*Dfz2*^{C1} *pip*^{1} *pip*^{2}	
Region 77	*Df(3L)XS-533* *Df(3L)rdgC-co2*	*Df(3L)XS-543*	*psn*^{B3} *psn*^{C4}	
Region 87	*Df(3R)T-32* *Df(3R)ry615*	*Df(3R)l26c* *Df(3R)ry75* *Df(3R)urd* *Df(3R)lc4a*		
Region 92	*Df(3R)Cha7* *Df(3R)Dl-BX12* *Df(3R)H-B79*	*Df(3R)Dl-A143*	*Dl*^{3}	

Six cytological regions selected after the primary screen were further investigated by testing smaller deficiencies and point mutations. Deficiencies and mutations that interact are underlined. Details about the strength of the interaction and the cytological positions for mutations and aberrations are in the APPENDIX.

This inversion is still present in *Df(3L)Scf-R6* and since one of the breakpoints is very close to where *dally* maps, the *dally* gene might be rearranged in this chromosome. Also, the complementation tests (see above) show that *dally*^{P2} (*l(3)06464*), as well as two *P* elements inserted distal and proximal to this gene [*l(3)01629* and *l(3)10534*, respectively], do not complement *Df(3L)Scf-R6*. Together, these observations suggest that *Df(3L)Scf-R6* is also a null for *dally*.

We tested three mutants in *dally*, *dally*^{10} (gift from Steve Kerridge), *dally*^{E285} (MERABET *et al.* 2002), and *dally*^{P2} (also named *l(3)06464*) (NAKATO *et al.* 1995). We found that two of these alleles, *dally*^{10} and *dally*^{E285}, gave a similar percentage of embryos with gaps as the overlapping deficiencies, 10.1% ($n = 238$) and 6.3% ($n = 221$), respectively. *dally*^{P2} is a *P*-element insertion thought to be a hypomorphic allele of *dally* (TSUDA *et al.* 1999) and does not interact in the screen. Taken together, these results suggest that *dally* is responsible for the interaction detected in the screen. This was verified later by RNAi silencing of *dally* in *enGal4/UASwg* embryos (see below).

Region 72: In the primary screen, we found one deficiency interacting in this region, *Df(3L)brm11*: 5.7% ($n = 157$). A smaller deficiency overlapping distally, *Df(3L)A27*, did not interact, whereas a deficiency overlapping proximally, *Df(3L)th102*, did, with a higher percentage of embryos with gaps: 18.6% ($n = 156$). This suggested that this deficiency removed not only the first locus found in the primary screen, but also a second interactor. Among other genes, we tested *brahma* (*brm*) and *notum* in the screen. The rationale for testing *notum* is that it codes for a hydrolase thought to modify the two Drosophila glypicans, Dally and Dlp (GERLITZ and BASLER 2002; GIRALDEZ *et al.* 2002). One allele of *brm*, *brm*^{2}, interacted at a similar level as *Df(3L)brm11*: 7.3% ($n = 150$). Two weaker alleles, *brm*^{T362} and *brm*^{T485}, did not interact. This suggests that *brm* is responsible for the interactions detected with *Df(3L)brm11*. We tested two alleles of *notum* and found that both interact (*not*^{3}, 17%, $n = 112$; *not*^{5}, 8.3%, $n = 96$), suggesting that *notum* is the second interacting locus removed by *Df(3L)th102*.

Region 75: Df(3L)VW3 interacted in the primary screen with 5.2% of embryos with gaps ($n = 134$). We tested a small deficiency on the distal side, *Df(3L)fz2*, and found a similar level of interaction: 8.0% ($n = 209$). This

deficiency removes *fz2*, and we therefore tested the only mutant allele available for this gene, $fz2^{C1}$ (Chen and Struhl 1999). We did not detect an interaction with this allele. We also investigated *pipe*, a gene coding for a sulphotransferase, which is removed by *Df(3L)VW3*, but two presumed null mutant alleles, pip^{1} and pip^{2}, did not interact.

Region 77: In region 77, we had found two deficiencies in the primary screen, *Df(3L)ri-79c* and *Df(3L)rdgC-co2*. *Df(3L)ri-79c* interacted strongly (34.2%), but this was caused by a dominant phenotype due to loss of *kni* and was independent of the *enGal4/UASwg* background (see above). *Df(3L)rdgC-co2* interacted weakly: 5.4% (n = 149). We tested one possible candidate gene removed by this deficiency, *Presenilin* (*Psn*), but did not find an interaction with the two tested alleles, Psn^{B3} and Psn^{C4}. We found another deficiency in the region, *Df(3L)XS-543*, which showed a similar interaction to the primary screen deficiency: 7.6% (n = 144). However, another deficiency tested in the primary screen, *Df(3L)XS533*, which overlaps with a large part of both *Df(3L)XS-543* and *Df(3L)rdgC-co2*, did not interact, thus confusing the mapping of the interacting locus. Precisely mapped deficiencies will need to be generated in this region to pursue the mapping further.

Region 87: In region 87, we found one deficiency, *Df(3R)ry615*, that interacted very weakly in the primary screen (4.1%, n = 169). We then found three smaller deficiencies in the region that showed slightly higher levels of interaction: *Df(3R)ry75*: 8.3% (n = 120), *Df(3R) urd*; 8.8% (n = 113), and *Df(3R)l26C*: 9.2% (n = 129). A fourth deficiency in the area, *Df(3R)lc4a*, did not interact. Although the same level of interaction suggested a single locus interacting in region 87, the given cytological breakpoints for these four deficiencies did not allow us to isolate a small interacting genomic area, suggesting that either more than one locus interacts or the mapping of the breakpoints for these deficiencies is imprecise.

Region 92: In region 92, *Df(3R) Dl-BX12* was found to interact weakly in the primary screen: 6.0% (n = 116). Since this deficiency removed *Delta*, we tested one allele in the screen, Dl^{3}, but did not find an interaction. The overlapping proximal and distal deficiencies *Df(3R)Cha7* and *Df(3R)H-b79* did not interact in the screen, suggesting that the interacting locus is present in the central region of *Df(3R) Dl-BX12*. We tested one smaller deficiency that removed this central region, *Df(3R)Dl-A143*, but did not find an interaction.

Further investigation of the role of *dally*, *dally-like*, and *notum* in Wingless distribution: Of six regions selected after the primary screen, five (cytology 66, 72, 75, 77, and 87; see Table 2) were found to still interact in the secondary screen. This shows that although weak, the majority of the interactions detected in the primary screen were meaningful. For two of these regions (cytology 66 and 72), we identified three genes, *dally*, *brm*, and *notum*, for which at least one mutant allele interacted in our screen. Because *brm* is a transcriptional regulator, we assumed that it is more likely to regulate the expression of segmentation genes than the distribution of Wg (Tamkun *et al.* 1992; Collins and Treisman 2000). We thus focused on examining the effect of *notum* and *dally* on Wg distribution in the embryonic epidermis. Since *dally* has a close homolog, *dally-like*, we also analyzed its role in this process.

Dally: To verify the weak interaction detected with two alleles of *dally*, we silenced the gene by RNAi in the *enGal4/UASwg* background. We found that 44% (n = 43) of the *enGal4/UASwg* embryos injected with *dally* dsRNA exhibit gaps in the denticle belts, which confirms its interaction in the screen (compare Table 3 with Figure 4E). By contrast, none of the *enGal4/UASwg* embryos injected with buffer exhibited any gaps (Table 3), and they were indistinguishable from noninjected *enGal4/UASwg* embryos (Figure 4B). In the secondary and primary screen, deficiencies and mutants in *dally* interacted with percentages ranging from 6.3 to 10.1% (appendix). Because only half of the embryos examined in the screen are actually mutant or deficient for *dally*, 12–20% of *enGal4/UASwg* embryos heterozygous for a *dally* mutation should exhibit patches of naked cuticle. Knocking down both zygotic and maternal *dally* mRNAs with RNAi in *enGal4/UASwg* embryos significantly increases this proportion (44%) as expected if *dally* is responsible for the interaction. However, we did not find any *enGal4/UASwg[dally RNAi]* embryos exhibiting the "full" phenotype found in *enGal4/UASwg* [hh^{-}/hh^{-}] embryos, where a symmetric expanse of naked cuticle is produced anterior as well as posterior to the Engrailed domain (Table 3 and Figure 4C) (Sanson *et al.* 1999). This is expected if *dally* is not the only factor that regulates Wg gradient formation in embryos.

The phenotype of excess naked cuticle seen in *enGal4/UASwg[dally RNAi]* embryos seems to occur independently of a major role for *dally* in segmentation. Indeed, *dally* RNAi in a wild-type background does not cause segmentation phenotypes at a frequency significantly different from buffer-injected controls (Desbordes and Sanson 2003). This is exemplified by the control in the experiment presented here: half of the embryos injected were of the *enGal4/TM3GFP* genotype (and thus wild type) and were identified by GFP expression (the other half of the embryos were *enGal4/UASwg*). Both buffer-injected and *dally* dsRNA-injected *enGal4/TM3GFP* embryos showed a similar proportion of segmentation defects, 23 and 21%, respectively (Table 3). These segmentation defects are very weak, consisting of occasional fusions or deletions of denticle belts, and they are a consequence of the injection process (Desbordes and Sanson 2003).

In conclusion, these experiments confirm that *dally* is the gene responsible for the interaction detected in the screen and suggest that its loss affects the distribu-

TABLE 3

RNAi silencing of *dally* and *dally-like* in *enGal4/UASwg* embryos

	enGal4/UASwg embryos[a]				*enGal4/TM3GFP* embryos[d]	
			Ectopic naked cuticle[c]			
	N	Segmentation defects[b]	Gap phenotype	Full phenotype	*N*	Segmentation defects[e]
Buffer	54	5 (9)	0	0	60	14 (23)
*dally ds*RNA	43	1 (2)	19 (44)	0	42	9 (21)
*dlp ds*RNA	61	23 (38)	9 (15)	24 (39)	71	58 (82)

enGal4 males were crossed to *UASwg/TM3GFP* females and embryos from the cross were injected with buffer, *dally* dsRNA, or *dlp* dsRNA. Embryos were separated in two groups at the end of embryogenesis on the basis of their GFP fluorescence, and their cuticle was examined. Numbers in parentheses are percentages.

[a] The nonfluorescent embryos are of genotype *enGal4/UASwg*. Different phenotypes were found.

[b] In all experiments, a proportion of embryos exhibited very weak segmentation defects, which is expected from damage due to the injection process (see Desbordes and Sanson 2003). However, *enGal4/UASwg[dlp RNAi]* embryos showed a proportion of segmentation defects significantly higher than the same embryos injected with buffer or *dally* dsRNA. Most of these segmentation defects were strong segment polarity phenotypes, suggesting that *dlp* has another role in segmentation in addition to its requirement for Hh signaling (see text).

[c] A significant proportion of *enGal4/UASwg* embryos injected with either *dally* or *dlp* dsRNA showed ectopic naked cuticle. In both experiments, embryos were found with patches of naked cuticle in the ventral denticle belts (gap phenotype), which was the phenotype looked for in the screen (see Figure 4E). A significant proportion of *enGal4/UASwg[RNAi dlp]* embryos also showed a phenotype identical to *enGal4/UASwg[hh-/hh-]* embryos, *i.e.*, naked cuticle on both sides of the Wg source (full phenotype) (see Figure 4D).

[d] The fluorescent embryos are of genotype *enGal4/TM3GFP* and thus show a wild-type cuticle pattern.

[e] As shown in Desbordes and Sanson (2003), injection of buffer or *dally* dsRNA gives a similar proportion of embryos with very weak segmentation defects, which are due to the injection process. By contrast, most wild-type embryos injected with *dlp* dsRNA exhibit strong segment polarity phenotypes, as expected from the failure in Hh signaling following *dlp* RNAi (Desbordes and Sanson 2003).

tion of Wg protein in wild-type embryos, without having a detectable effect on Wg signaling *per se*.

Dally-like: At the time we did this work, no mutations were available in *dlp*, so we tested a potential interaction in our screen by RNAi silencing in the *enGal4/UASwg* background. We found that 54% ($n = 61$) of the *enGal4/UASwg[dlp RNAi]* embryos showed excess naked cuticle in the abdominal segments (whereas *enGal4/UASwg* embryos injected with buffer showed no phenotype) (Table 3). Of these 54%, 15% showed gaps in the denticle belts, which was the phenotype looked for in the screen and is similar to the phenotype seen in *enGal4/UASwg [hh$^-$/+]* embryos. Moreover, 39% showed the same phenotype as *enGal4/UASwg [hh$^-$/hh$^-$]* embryos, *e.g.*, a symmetric expanse of naked cuticle anterior and posterior to the Engrailed domain (Table 3 and Figure 4, C *vs.* D). This suggested that the Wg gradient had become symmetric in these embryos. To demonstrate that the cuticle phenotype seen in *enGal4/UASwg[dlp RNAi]* embryos was due to a change in Wg protein distribution, we stained stage 12 embryos with a Wg antibody (Figure 5). While in *enGal4/UASwg* embryos, Wg protein is never detected posterior to the En domain (Sanson *et al.* 1999); in *enGal4/UASwg[dlp RNAi]* embryos, Wg is detected both anterior and posterior to the En domain (Figure 5, E–E′′′). This symmetric distribution is identical to the distribution observed in *enGal4/UASwg[hh$^-$/hh$^-$]* embryos (Sanson *et al.* 1999). The symmetric distribution in *enGal4/UASwg[dlp RNAi]* can be explained in two ways: either *dlp* regulates Wg distribution directly, downstream of Hh signaling, or *dlp* regulates Hh signaling, and thus affects Wg distribution indirectly, through Hh. We found that the latter hypothesis is correct. In *enGal4/UASwg[hh$^-$/hh$^-$]* embryos, endogenous *wg* expression is lost, because Hh signaling is absent and the maintenance of *wg* transcription fails (Figure 5, B′ *vs.* C′). If Dlp were regulating Wg distribution directly, without affecting Hh signaling, *wg* endogenous expression would be maintained in *enGal4/UASwg[dlp RNAi]* embryos. We found that this is not the case: *wg* endogenous expression disappears in *enGal4/UASwg[dlp RNAi]* embryos as in *enGal4/UASwg[hh$^-$/hh$^-$]* embryos (Figure 5, C and D), suggesting that Dlp is required for either Hh expression or signaling. We demonstrated elsewhere by additional experiments that Dlp is strictly required for Hh signaling in the embryonic epidermis (Desbordes and Sanson 2003).

We also looked at the effect of *dlp* RNAi in a wild-type background. In contrast to *dally* RNAi, *dlp* RNAi causes a full segment polarity phenotype (Desbordes and Sanson 2003). This is found as well in the experiment presented here: 82% ($n = 71$) of the control embryos, *enGal4/TM3GFP*, exhibit segmentation defects when injected with *dlp* dsRNA (Table 3). Contrary to

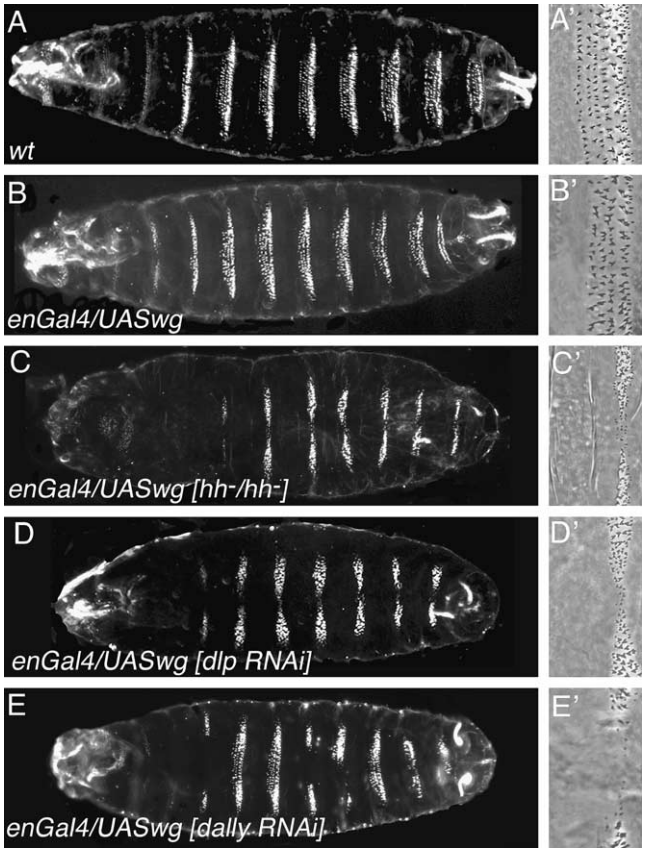

FIGURE 4.—*dally-like* or *dally* RNAi in *enGal4/UASwg* embryos produces ectopic naked cuticle posterior to the Wingless source. (A) Wild-type larva and (A′) close-up of abdominal denticle belt. Denticle rows 1–6 are visible. (B) *enGal4/UASwg* larva: row 1 is completely or partially missing in denticle belts of abdominal segments A2–A7. (B′) Close-up showing a belt where row 1 is missing completely. Rows 2–6 are intact. (C) *enGal4/UASwg[hh⁻/hh⁻]* embryo: an identical expanse of naked cuticle is found posterior and anterior to the Wg source. (C′) Close-up showing that rows 2–5 have been replaced by naked cuticle. (D) *enGal4/UASwg[dlp RNAi]* embryo and close-up (D′) showing a very similar phenotype to *enGal4/UASwg[hh⁻/hh⁻]* embryos. (E and E′) *enGal4/UASwg[dally RNAi]* embryo shows an intermediate phenotype with ectopic naked cuticle in some of the denticle belts.

what is seen in embryos injected with buffer or *dally* dsRNA, most of these segmentation defects are actually strong segment polarity phenotypes, identical to the phenotypes seen in *wg* or *hh* loss of function (not shown; see DESBORDES and SANSON 2003). On the basis of our study in DESBORDES and SANSON (2003), which shows that Dlp is required for Hh signaling, and the evidence from Figure 5, we conclude that the dramatic change of Wg distribution found in *enGal4/UASwg[dlp RNAi]* embryos is (at least in part) the indirect consequence of loss of Hh signaling.

It is worth noting that *enGal4/UASwg[RNAi dlp]* embryos do not have a phenotype strictly identical to *enGal4/UASwg[hh⁻/hh⁻]* embryos. Ectopic *wg* transcription in *enGal4/UASwg[RNAi dlp]* embryos is less robust than that in *enGal4/UASwg[hh⁻/hh⁻]* embryos (Figure 5, C and C′ *vs.* D and D′). This suggests that *en* maintenance might be impaired in *dlp* RNAi embryos. Moreover, in *enGal4/UASwg[RNAi dlp]* embryos, 38% exhibit segmentation defects, whereas the rest exhibit excess naked cuticle (Table 3). Most of these segmentation defects are strong segment polarity phenotypes, suggesting that normal segmentation fails in these embryos, despite the presence of the artificial autoregulatory loop between *en* and *wg*. A possibility is that Dlp affects Wg signaling in addition to being required for Hh signaling (see DISCUSSION).

Notum: The two tested alleles of *notum*, not^3 and not^5, interact unambiguously in our screen. The interaction with not^3 is stronger than that with not^5 (17.0 *vs.* 8.3%; see APPENDIX), which is consistent with the characterization of not^3 and not^5 as amorphic and hypomorphic, respectively (GIRALDEZ *et al.* 2002). We looked at the phenotype of these mutations in a wild-type background. not^5 is homozygous viable so we were able to look at embryos mutant for the zygotic and maternal contribution of the gene (*i.e.*, embryos derived from not^5/not^5 mothers). We found that 85% ($n = 85$) of the embryos have row 1 missing in most denticle belts and often have a breach of naked cuticle in segment A1. Ten percent of the embryos have stronger phenotypes, with patches of naked cuticle within denticle belts and sometimes complete replacement of denticle belts by naked cuticle (Figure 6A). Similar phenotypes, albeit weaker, were observed in not^3/not^3 embryos derived from heterozygous mothers (the not^3 chromosome is homozygous embryonic lethal). The presence of a wild-type maternal contribution in not^3/not^3 embryos could account for the weaker phenotype. To test this, we examined embryos from mothers bearing germline clones homozygous for the not^3 mutant chromosome. Germline clones bearing females were crossed with $not^3/TM3GFP$ males to generate embryos both maternally and zygotically mutant for *notum*. The GFP-expressing embryos, which have a wild-type copy of *notum* contributed paternally, hatched and did not show any obvious phenotype. The embryos that do not express GFP, and thus are maternally and zygotically mutants for *notum*, exhibit a range of severe defects. First, most of the mutants have an abnormal morphology. For example, out of a collection of 76 mutant embryos, 33 (43%) have a posterior end that is not completely retracted, 9 (12%) are U-shaped, and 26 (34%) are shaped like a ball (Figure 6, B–B″). These phenotypes suggest an early requirement of *notum* in patterning and/or morphogenesis, which we have not attempted to characterize here. We could not analyze reliably the ventral cuticle pattern of U-shaped or ball-shaped embryos, but we analyzed it for the 41 remaining embryos: all except one showed thinner denticle belts in the abdomen, and in addition, 16 embryos showed either gaps of naked cuticle in the belts or missing belts (Figure 6B″). Thus the majority

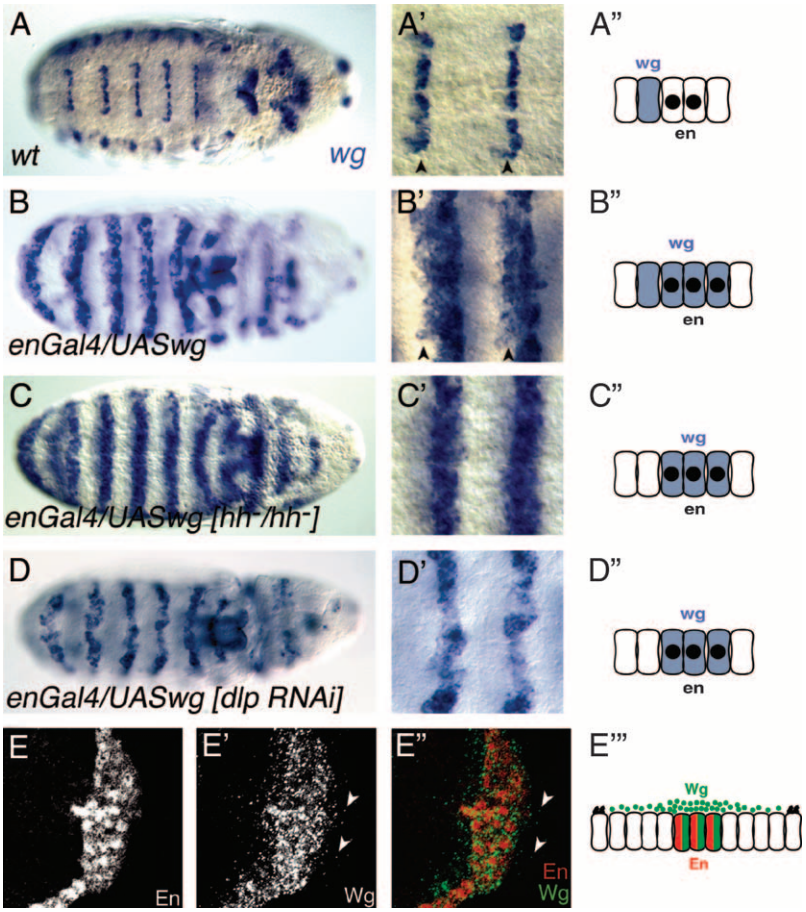

FIGURE 5.—The symmetrical Wingless gradient in *enGal4/UASwg[dlp RNAi]* embryos is a consequence of loss of Hedgehog signaling. (A–D) *wg* trancription revealed by *in situ* hybridization in late stage 11 embryos. Embryos are voluntarily oriented with the head to the right, to keep the anterior side of each segment to the left, as in the close-up views and the diagrams. (A–A′′) In wild-type embryos, *wg* is transcribed in a single row of cells in each segment, just anterior to the En-expressing cells. (B–B′′) In *enGal4/UASwg* embryos, *wg* is transcribed ectopically in the En domain, which occupies two to three rows of cells in each segment. The endogenous expression of *wg* is visible as a row of cells immediately anterior to the domain of ectopic *wg* expression (arrowheads in B′). It is possible to distinguish unambiguously ectopic from endogenous *wg* expression without double label, because endogenous *wg* expression is restricted at this stage to the ventral cells, whereas ectopic *wg* expression in the En domain spans the circumference of the embryo. (C–C′′) In a *hh* null mutant background, ectopic *wg* expression is maintained in *enGal4/UASwg* embryos, because the regulatory loop created between En and Wg bypasses the need for Hh signaling. However, outside of the En domain, endogenous *wg* expression still requires Hh for its maintenance and is consequently lost in these embryos (no ventral stripe of endogenous *wg* expression is seen). (D–D′′) Endogenous *wg* expression is also lost in *enGal4/UASwg[dlp RNAi]* embryos, suggesting that Hh signaling has failed in these embryos. If Hh signaling is normal, *wg* endogenous expression should be maintained. Note that *wg* ectopic transcription in the Engrailed domain is not as robust as in *enGal4/UASwg[hh⁻/hh⁻]* embryos. (E–E′′′) Wg protein distribution in *enGal4/UASwg[dlp RNAi]* embryos. The En domain is labeled in red and Wg protein in green in the merge (E′′). Wg protein is detected posterior, as well as anterior to the En domain, in dots (arrowheads). This shows that the Wg gradient is symmetric in *enGal4/UASwg[dlp RNAi]* embryos (E′′′), contrary to *enGal4/UASwg* embryos where the Wg gradient is asymmetric (see Figure 1 and also SANSON *et al.* 1999; DUBOIS *et al.* 2001).

of embryos for which the cuticle pattern can be analyzed showed ectopic naked cuticle in the abdominal segments. These phenotypes are similar, albeit much more severe, than those found for the hypomorphic not^5 mutant.

To test if the phenotype of ectopic naked cuticle was due to a change in Wg distribution, we stained not^3 mutant embryos with a Wg antibody. Females bearing not^3 germline clones were crossed with males not^3/*TM3LacZ*, using LacZ to distinguish the paternally rescued embryos from the not^3 mutant embryos. Both paternally rescued and not^3 mutant embryos were stained together to enable us to compare the intensity of staining for the Wg protein (Figure 6). Strikingly, at stages 12 and 13 Wg staining in *notum* mutant embryos appears weaker and more diffuse than that in paternally rescued embryos (Figure 6, C and C′ *vs.* D and D′). In paternally rescued embryos, most of the staining is concentrated on a single row of cells immediately anterior to the Engrailed-expressing cells, as in wild-type embryos (Figure 6, C and C′, and not shown; see also SANSON *et al.* 1999). By contrast, in not^3 mutant embryos, Wg staining is weaker overall and appears to span two to three cell diameters rather than one (Figure 6, D and D′). This experiment indicates that either *wingless* is transcribed in a broader domain and less actively or the shape of the Wg gradient is altered in not^3 mutant embryos.

DISCUSSION

A screen for genes required for Wingless gradient formation: We found six regions interacting as deficiencies in our screen, and from these we isolated the genes *brm*, *dally*, and *notum* as interactors. Since we completed the screen, *dally* and *notum* have been found to affect Wg distribution, respectively, in cell culture (LUM *et al.* 2003; FRANCH-MARRO *et al.* 2005) and in the wing imaginal disc (GIRALDEZ *et al.* 2002), thus validating the ability of our screen to find genes regulating the Wg gradient.

We did not find any genes that gave a dominant phenotype as penetrant as *hh* in our sensitized background. The interactions detected are weak, which suggests that a combination of factors rather than a single one regu-

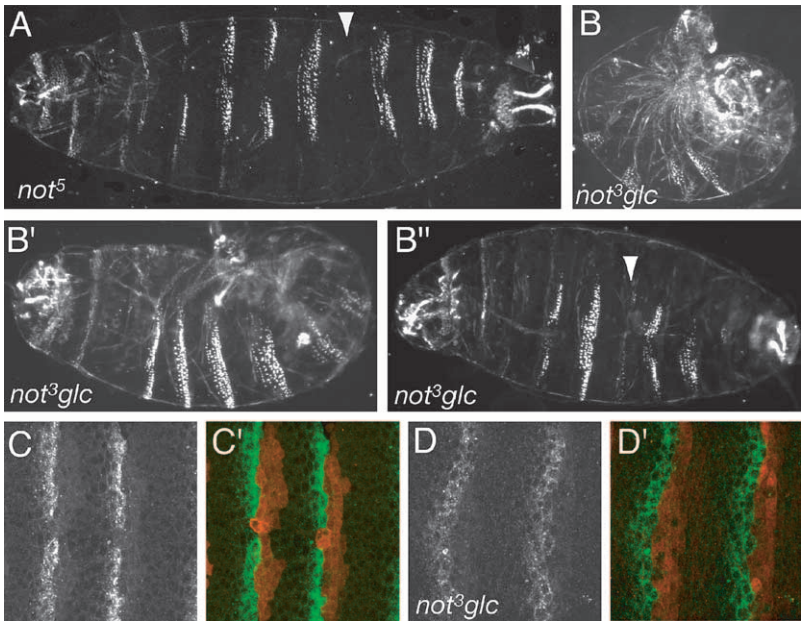

FIGURE 6.—Embryos mutant for *notum* show ectopic naked cuticle and a broader Wg gradient. (A) *not*^{5} embryo showing excess naked cuticle in segments A1, A2, A3, A5, and A6. Note that the denticle belt in segment A5 has been completely replaced by naked cuticle (arrowhead). (B–B′′) Embryos derived from *not*^{3} germline clones; *i.e.*, embryos both maternally and zygotically mutant for *notum* exhibit a range of cuticle defects. Some embryos are ball shaped (B) or U shaped (B′), while others have an incompletely retracted posterior end (B′′). In addition, most embryos for which the cuticle pattern can be analyzed show a narrowing of the ventral denticle belts, with patches of naked cuticle in the belts or denticle belts missing (arrowhead in B′′). (C and D) Stage 12 embryos derived from females bearing *not*^{3} germlines clones and *not*^{3}*/TM3LacZ* males were stained for Wg (C and D and green signal in C′ and D′). These embryos also carry *enGal4.UASGFP* to label the *engrailed* domain using an antibody against GFP (red signal in C′ and D′). LacZ-positive embryos are paternally rescued and show a Wg gradient indistinguishable from wild-type embryos (C and C′). LacZ-negative embryos are maternally and zygotically mutant for *notum* and show a Wg gradient that is broader and weaker (D and D′).

late the shape of the Wg gradient in embryos, downstream of Hh signaling. It also seems likely that most factors involved are maternally provided, as is the case for *dally* and *notum*. Our screen did not remove any maternal contribution since we tested heterozygous males for a given deficiency chromosome, due to the constraints in the reagents available at the time (see MATERIALS AND METHODS). Hence, the wild-type maternal contribution would weaken the interactions detected for genes contributed maternally and zygotically, such as *dally* and *notum*. This can also explain why not all the mutant alleles tested for *dally* interact: weak modifiers present elsewhere on the third chromosome of mutant alleles might be enough to mask an interaction already diminished by the maternal contribution.

However, although weak, most interactions detected in our primary screen were confirmed in the secondary screen and we believe that it can be applied to the whole genome to find additional factors regulating Wg gradient formation. In light of our results, two changes could be made to improve screen efficiency. First, females heterozygous for a given deficiency, instead of males, could be used to remove half of the maternal contribution in addition to halving the zygotic contribution (note that F_1 *UASwg/+; Deficiency/+* females should be used rather than *enGal4/+; Deficiency/+* females, since the progeny of the latter display an interfering phenotype; see MATERIALS AND METHODS). This should uncover maternal factors that might have been overlooked in our screen. Second, the use of precisely mapped deficiencies from the new Drosdel collection (RYDER *et al.* 2004), instead of the current deficiency collection, should improve dramatically the mapping of the interactors. Indeed, the current deficiency kit does not cover the whole genome and many deficiencies either are imprecisely mapped or represent complex aberrations [such as Df(3L)ScfR6], which renders analysis difficult. Also, the current deficiency kit contains some very large deficiencies, which might not interact because they remove modifiers. Another problem with large deficiencies is that some are haplo-insufficient and could not be tested in the screen because heterozygous males did not survive or were sterile.

Another use of the *enGal4/UASwg*-sensitized background is to test the role of candidate genes in Wg gradient formation. For example, *deep orange* (*dor*) and *Chlathrin* (*Chc*), two genes required for lysosomal degradation, have already been found to produce ectopic naked cuticle when their zygotic contribution is removed in the *enGal4/UASwg* background (DUBOIS *et al.* 2001). This contributed to the demonstration that Wg is degraded at a faster rate posterior to the En domain. It is worth noting that *dor* and *Chc* zygotic mutants do not exhibit any cuticle phenotype and thus do not reveal their role in Wg distribution without the sensitized background. Moreover, the maternal contribution of *dor* and *Chc* cannot be removed genetically in the maternal germline, since these genes are required for oogenesis. Thus the use of the *enGal4/UASwg* background provides an assay for genes that could not be tested otherwise in embryonic gradient formation.

Role of Dally-like in Wingless gradient formation: RNAi silencing of *dally* or *dlp* in *enGal4/UASwg* embryos generated ectopic naked cuticle in both cases, but *dlp* silencing had a much stronger effect (Figure 4 and Table 3). This strong phenotype is explained at least in

part by the strict requirement for Dlp in Hh signaling (Desbordes and Sanson 2003) (Figure 5). In *enGal4/UASwg [dlp RNAi]* embryos, the failure of Hh signaling generates a symmetrical gradient of Wg protein and results in a phenotype identical to *enGal4/UASwg [hh⁻/hh⁻]* embryos (Figure 5) (Sanson *et al.* 1999).

Dlp could be regulating Wg distribution as well, but its requirement for Hedgehog signaling makes this difficult to assess. We noted, however, that a significant proportion of *enGal4/UASwg [dlp RNAi]* embryos shows a segment polarity phenotype (Table 3) and that the stripe of *wg* transcription in the *en* domain of these embryos is weak compared to the control *enGal4/UASwg [hh⁻/hh⁻]* embryos (Figure 5, C and C′ *vs.* D and D′). The simplest way to explain these phenotypes is if *en* expression is somewhat compromised in *enGal4/UASwg [dlp RNAi]* embryos. Surprisingly, this effect would be specific to *en*, since naked cuticle can still form in the absence of *dlp* (Figure 4D) (Desbordes and Sanson 2003; Franch-Marro *et al.* 2005). It is possible that in contrast to naked cuticle specification, En maintenance requires high levels of Wg. In support of this idea, only the cells immediately adjacent to the Wg-expressing cells are able to maintain En expression at stage 10 (Vincent and Lawrence 1994). Thus, it is possible that Dlp is required to maintain a high concentration of Wg at the surface of the Wg-expressing cells and that this contributes to the maintenance of En expression in adjoining cells. In the absence of Dlp, Wg would be released from the cells, thus compromising En maintenance without affecting naked cuticle specification (this might even promote naked cuticle specification over a longer distance). Consistent with this hypothesis, very recent results show that in the wing disc Dlp has opposite effects on short-range and long-range Wg signaling (Kirkpatrick *et al.* 2004; Kreuger *et al.* 2004; Franch-Marro *et al.* 2005).

Role of Dally in Wingless gradient formation: The excess naked cuticle observed in *enGal4/UASwg [dally RNAi]* embryos could be due to a partial requirement in Hh signaling or, alternatively, to a direct effect on Wg distribution. Both hypotheses are plausible since Dally is required redundantly with Dlp for Hh signaling in wing discs (Han *et al.* 2004a) and recent data indicate that Dally can affect Wg distribution (Lum *et al.* 2003; Franch-Marro *et al.* 2005). In Drosophila cultured cells, Dally transfection causes accumulation of exogenous Wg at the cell surface (Franch-Marro *et al.* 2005), whereas *dally* RNAi results in loss of Wg staining (see note 20 in Lum *et al.* 2003). Taken together, these observations suggest that Dally is able to retain Wg protein at the cell surface. It may be that, in the embryo, loss of *dally* releases Wg and allows it to signal at a longer range to make naked cuticle.

This effect of Dally seems to be independent of a requirement for Wg signaling *per se*, since embryos either depleted of *dally* mRNA following RNAi (this study and Desbordes and Sanson 2003) or zygotically and maternally mutant for *dally* (Franch-Marro *et al.* 2005) do not exhibit any segment polarity phenotype. However, Dally might cooperate with Dlp to modulate Wg signaling because embryos mutant for both *dally* and *dlp* have a stronger segment polarity phenotype than *hh* mutants (Dlp is strictly required for Hh signaling) and phenocopy the phenotype of *wg hh* double mutants (Franch-Marro *et al.* 2005).

Role of Notum in Wingless gradient formation: Halving the dose of *notum* in *enGal4/UASwg* embryos generates ectopic naked cuticle (appendix). Moreover, *notum* mutants exhibit variable amounts of excess naked cuticle (Figure 6) (see also Giraldez *et al.* 2002). Consistent with this effect, overexpression of Notum in embryos inhibits the formation of naked cuticle (Giraldez *et al.* 2002). We found that in embryos maternally and zygotically mutant for *notum*, the Wg gradient appears broader than in wild-type embryos (Figure 6, D and D′). This broadening is seen clearly for the anterior Wg gradient, whereas it is less easy to observe posterior to the Wg source. This is expected if the fast degradation of Wg occurring posterior to the source (Dubois *et al.* 2001) is operating normally in *notum* mutants, thus masking changes in the distribution of Wg protein. We suggest that in *notum* mutants more Wg is available for signaling before it is targeted for degradation, resulting in the formation of ectopic naked cuticle posterior to the Wg source. A broadening of the Wg gradient has also been found for *notum* mutant clones in the wing disc (Giraldez *et al.* 2002). In contrast to what has been observed in the wing disc, however, the broader Wg gradient in *notum* mutant embryos also appears weaker (Figure 6, D and D′). This does not seem to have an impact on signaling, however, since no segment polarity phenotypes were observed in *notum* mutant embryos, suggesting that *engrailed* maintenance is normal.

Notum has homologies to pectin acetylesterases and appears to modify the activity of glypicans, in particular Dlp (Gerlitz and Basler 2002; Giraldez *et al.* 2002). Recent work indicates that Notum directly or indirectly induces cleavage of the glycosylphosphatidylinositol anchor of Dlp (but not Dally), leading to shedding of this glypican from the cell surface (Kreuger *et al.* 2004). It has been hypothesized that Wg bound to Dlp could be made unavailable to signaling because of shedding from the cell surface, thus explaining the increase in Wg activity associated with loss of Notum. What is the substrate of Notum in the embryo? In the epidermis, both *notum* and *dlp* are upregulated in the cells that respond to Wg (Khare and Baumgartner 2000; Giraldez *et al.* 2002). By contrast, *dally* is downregulated in the same cells, suggesting that Wg signaling might repress *dally* expression (Tsuda *et al.* 1999). This could reflect a different or even opposite role of the two glypicans in Wg gradient formation. Since in the wing disc Notum appears to act on Dlp and not Dally, the effects that we

observe could be attributed to the regulation of Dlp by Notum. If this is true, this would reveal a role for Dlp in Wg gradient formation in the embryo, in addition to its role in Hh signaling. Interestingly, in addition to changes in the cuticle pattern, loss of *notum* causes severe defects in the patterning and/or morphogenesis of the early embryo (Figure 6), suggesting that Notum may have substrates other than the glypicans.

We thank Clive McKimmie for his early contribution to the screen, Margit Pál for the *in situ* hybridizations on polytene chromosomes, Daniel St. Johnston and Jean-Paul Vincent for their comments on the manuscript, and Francois Balloux for advice on the statistics. We also thank K. Cadigan, S. Cohen, M. Fortini, D. Kalderon, S. Kerridge, D. St Johnston, G. Struhl, J. Treisman, the Hybridoma Bank, the Bloomington and Umea stock centers, and FlyBase for fly strains, reagents, and valuable information. This work was supported by a Career Development Award from the Wellcome Trust (054525/Z/98) to B.S. B.S. was also supported by the Cambridge Newton Trust and S.D. by the Cambridge European Trust.

LITERATURE CITED

Baeg, G. H., X. Lin, N. Khare, S. Baumgartner and N. Perrimon, 2001 Heparan sulfate proteoglycans are critical for the organization of the extracellular distribution of Wingless. Development **128:** 87–94.

Bejsovec, A., and E. Wieschaus, 1995 Signaling activities of the Drosophila wingless gene are separately mutable and appear to be transduced at the cell surface. Genetics **139:** 309–320.

Bellaiche, Y., I. The and N. Perrimon, 1998 Tout-velu is a Drosophila homologue of the putative tumour suppressor EXT-1 and is needed for Hh diffusion. Nature **394:** 85–88.

Cadigan, K. M., M. P. Fish, E. J. Rulifson and R. Nusse, 1998 Wingless repression of Drosophila frizzled 2 expression shapes the Wingless morphogen gradient in the wing. Cell **93:** 767–777.

Carroll, S. B., and M. P. Scott, 1986 Zygotically active genes that affect the spatial expression of the fushi tarazu segmentation gene during early Drosophila embryogenesis. Cell **45:** 113–126.

Chen, C. M., and G. Struhl, 1999 Wingless transduction by the Frizzled and Frizzled2 proteins of Drosophila. Development **126:** 5441–5452.

Chen, Y., and G. Struhl, 1996 Dual roles for patched in sequestering and transducing Hedgehog. Cell **87:** 553–563.

Collins, R. T., and J. E. Treisman, 2000 Osa-containing Brahma chromatin remodeling complexes are required for the repression of wingless target genes. Genes Dev. **14:** 3140–3152.

Cox, R. T., D. G. McEwen, D. L. Myster, R. J. Duronio, J. Loureiro *et al.*, 2000 A screen for mutations that suppress the phenotype of *Drosophila armadillo*, the β-catenin homolog. Genetics **155:** 1725–1740.

Desbordes, S., 2004 The role of the Drosophila glypicans in Wingless and Hedgehog signalling during embryogenesis. Ph.D. Thesis, University of Cambridge, Cambridge, UK.

Desbordes, S. C., and B. Sanson, 2003 The glypican Dally-like is required for Hedgehog signalling in the embryonic epidermis of Drosophila. Development **130:** 6245–6255.

Dougan, S., and S. DiNardo, 1992 Drosophila wingless generates cell type diversity among engrailed expressing cells. Nature **360:** 347–350.

Dubois, L., M. Lecourtois, C. Alexandre, E. Hirst and J. P. Vincent, 2001 Regulated endocytic routing modulates wingless signaling in Drosophila embryos. Cell **105:** 613–624.

Franch-Marro, X., O. Marchand, E. Piddini, S. Ricardo, C. Alexandre *et al.*, 2005 Glypicans shunt the Wingless signal between local signalling and further transport. Development **132:** 659–666.

Freeman, M., 2000 Feedback control of intercellular signalling in development. Nature **408:** 313–319.

Gerlitz, O., and K. Basler, 2002 Wingful, an extracellular feedback inhibitor of Wingless. Genes Dev. **16:** 1055–1059.

Giraldez, A. J., R. R. Copley and S. M. Cohen, 2002 HSPG modification by the secreted enzyme Notum shapes the Wingless morphogen gradient. Dev. Cell **2:** 667–676.

Gonzalez, F., L. Swales, A. Bejsovec, H. Skaer and A. Martinez Arias, 1991 Secretion and movement of wingless protein in the epidermis of the Drosophila embryo. Mech. Dev. **35:** 43–54.

Gonzalez-Gaitan, M., 2003 Endocytic trafficking during Drosophila development. Mech. Dev. **120:** 1265–1282.

Greco, V., M. Hannus and S. Eaton, 2001 Argosomes: a potential vehicle for the spread of morphogens through epithelia. Cell **106:** 633–645.

Han, C., T. Y. Belenkaya, B. Wang and X. Lin, 2004a Drosophila glypicans control the cell-to-cell movement of Hedgehog by a dynamin-independent process. Development **131:** 601–611.

Han, C., T. Y. Belenkaya, M. Khodoun, M. Tauchi and X. Lin, 2004b Distinct and collaborative roles of Drosophila EXT family proteins in morphogen signalling and gradient formation. Development **131:** 1563–1575.

Hatini, V., and S. DiNardo, 2001 Divide and conquer: pattern formation in Drosophila embryonic epidermis. Trends Genet **17:** 574–579.

Jowett, T., 1997 *Tissue in Situ Hybridization: Methods in Animal Development.* John Wiley & Sons, New York.

Khare, N., and S. Baumgartner, 2000 Dally-like protein, a new Drosophila glypican with expression overlapping with wingless. Mech. Dev. **99:** 199–202.

Kirkpatrick, C. A., B. D. Dimitroff, J. M. Rawson and S. B. Selleck, 2004 Spatial regulation of Wingless morphogen distribution and signaling by Dally-like protein. Dev. Cell **7:** 513–523.

Kopp, A., and I. Duncan, 1997 Control of cell fate and polarity in the adult abdominal segments of Drosophila by optomotor-blind. Development **124:** 3715–3726.

Kreuger, J., L. Perez, A. J. Giraldez and S. M. Cohen, 2004 Opposing activities of Dally-like glypican at high and low levels of Wingless morphogen activity. Dev. Cell **7:** 503–512.

Lawrence, P. A., B. Sanson and J. P. Vincent, 1996 Compartments, wingless and engrailed: patterning the ventral epidermis of Drosophila embryos. Development **122:** 4095–4103.

Lecourtois, M., C. Alexandre, L. Dubois and J. P. Vincent, 2001 Wingless capture by Frizzled and Frizzled2 in Drosophila embryos. Dev. Biol. **235:** 467–475.

Lecuit, T., and S. M. Cohen, 1998 Dpp receptor levels contribute to shaping the Dpp morphogen gradient in the Drosophila wing imaginal disc. Development **125:** 4901–4907.

Lin, X., and N. Perrimon, 1999 Dally cooperates with Drosophila Frizzled 2 to transduce Wingless signalling. Nature **400:** 281–284.

Lindsley, D. L., and G. Zimm, 1992 *The Genome of Drosophila melanogaster.* Academic Press, New York.

Lum, L., S. Yao, B. Mozer, A. Rovescalli, D. Von Kessler *et al.*, 2003 Identification of Hedgehog pathway components by RNAi in Drosophila cultured cells. Science **299:** 2039–2045.

Merabet, S., F. Catala, J. Pradel and Y. Graba, 2002 A green fluorescent protein reporter genetic screen that identifies modifiers of Hox gene function in the Drosophila embryo. Genetics **162:** 189–202.

Moline, M. M., C. Southern and A. Bejsovec, 1999 Directionality of wingless protein transport influences epidermal patterning in the Drosophila embryo. Development **126:** 4375–4384.

Nakato, H., T. A. Futch and S. B. Selleck, 1995 The division abnormally delayed (dally) gene: a putative integral membrane proteoglycan required for cell division patterning during postembryonic development of the nervous system in Drosophila. Development **121:** 3687–3702.

Neumann, C. J., and S. M. Cohen, 1997 Long-range action of Wingless organizes the dorsal-ventral axis of the Drosophila wing. Development **124:** 871–880.

O'Keefe, L., S. T. Dougan, L. Gabay, E. Raz, B. Z. Shilo *et al.*, 1997 Spitz and Wingless, emanating from distinct borders, cooperate to establish cell fate across the Engrailed domain in the Drosophila epidermis. Development **124:** 4837–4845.

Payre, F., A. Vincent and S. Carreno, 1999 ovo/svb integrates Wingless and DER pathways to control epidermis differentiation. Nature **400:** 271–275.

Pfeiffer, S., C. Alexandre, M. Calleja and J. P. Vincent, 2000 The progeny of wingless-expressing cells deliver the signal at a distance in Drosophila embryos. Curr. Biol. **10:** 321–324.

Pfeiffer, S., S. Ricardo, J. B. Manneville, C. Alexandre and J. P. Vincent, 2002 Producing cells retain and recycle Wingless in Drosophila embryos. Curr. Biol. **12:** 957–962.

Reichsman, F., L. Smith and S. Cumberledge, 1996 Glycosaminoglycans can modulate extracellular localization of the wingless protein and promote signal transduction. J. Cell Biol. **135:** 819–827.

Ryder, E., F. Blows, M. Ashburner, R. Bautista-Llacer, D. Coulson *et al.*, 2004 The DrosDel collection: a set of *P*-element insertions for generating custom chromosomal aberrations in *Drosophila melanogaster*. Genetics **167:** 797–813.

Sanson, B., 2001 Generating patterns from fields of cells. Examples from Drosophila segmentation. EMBO Rep. **2:** 1083–1088.

Sanson, B., C. Alexandre, N. Fascetti and J. P. Vincent, 1999 Engrailed and hedgehog make the range of Wingless asymmetric in Drosophila embryos. Cell **98:** 207–216.

Seto, E. S., and H. J. Bellen, 2004 The ins and outs of Wingless signaling. Trends Cell Biol. **14:** 45–53.

Simmonds, A. J., G. dosSantos, I. Livne-Bar and H. M. Krause, 2001 Apical localization of wingless transcripts is required for wingless signaling. Cell **105:** 197–207.

St Johnston, D., and C. Nusslein-Volhard, 1992 The origin of pattern and polarity in the Drosophila embryo. Cell **68:** 201–219.

Strigini, M., and S. M. Cohen, 2000 Wingless gradient formation in the Drosophila wing. Curr. Biol. **10:** 293–300.

Takei, Y., Y. Ozawa, M. Sato, A. Watanabe and T. Tabata, 2003 Three Drosophila EXT genes shape morphogen gradients through synthesis of heparan sulfate proteoglycans. Development **131:** 73–82.

Tamkun, J. W., R. Deuring, M. P. Scott, M. Kissinger, A. M. Pattatucci *et al.*, 1992 brahma: a regulator of Drosophila homeotic genes structurally related to the yeast transcriptional activator SNF2/SWI2. Cell **68:** 561–572.

Tanimoto, H., S. Itoh, P. ten Dijke and T. Tabata, 2000 Hedgehog creates a gradient of DPP activity in Drosophila wing imaginal discs. Mol. Cell **5:** 59–71.

The, I., Y. Bellaiche and N. Perrimon, 1999 Hedgehog movement is regulated through tout velu-dependent synthesis of a heparan sulfate proteoglycan. Mol. Cell **4:** 633–639.

Tsuda, M., K. Kamimura, H. Nakato, M. Archer, W. Staatz *et al.*, 1999 The cell-surface proteoglycan Dally regulates Wingless signalling in Drosophila. Nature **400:** 276–280.

van den Heuvel, M., R. Nusse, P. Johnston and P. A. Lawrence, 1989 Distribution of the wingless gene product in Drosophila embryos: a protein involved in cell-cell communication. Cell **59:** 739–749.

Vincent, J. P., and L. Dubois, 2002 Morphogen transport along epithelia, an integrated trafficking problem. Dev. Cell **3:** 615–623.

Vincent, J. P., and P. A. Lawrence, 1994 Drosophila wingless sustains engrailed expression only in adjoining cells: evidence from mosaic embryos. Cell **77:** 909–915.

Zecca, M., K. Basler and G. Struhl, 1996 Direct and long-range action of a wingless morphogen gradient. Cell **87:** 833–844.

Communicating editor: K. V. Anderson

APPENDIX

Deficiencies and mutations tested in the primary and secondary screens

Deficiency	Cytology	% *enGal4/UASwg* embryos with gaps	Interaction
	Primary screen		
Df(3L)emc-E12	61A; 61D3	2.7 ($n = 111$)	No
Df(3L)Ar14-8	61C5-8; 62A8	1.6 ($n = 126$)	No
Df(3L)Aprt-1	62A10-B1; 62D2-5	1.7 ($n = 275$)	No
Df(3L)R-G7	62B9; 62E7	1.5 ($n = 136$)	No
Df(3L)HR119	63C2;63F7	3.3 ($n = 121$)	No
Df(3L)GN24	63F4-7;64C13-15	1.2 ($n = 86$)	No
Df(3L)ZN47	64C;65C	1.0 ($n = 98$)	No
Df(3L)XDI98	65A2;65E1	0.9 ($n = 109$)	No
Df(3L)pbl-X1	65F3;66B10	3.0 ($n = 101$)	No
Df(3L)66C-G28	66B8-9;66C9-10	0 ($n = 123$)	No
Df(3L)h-i22	66D1011;66E1-2	6.4 ($n = 249$)	Yes ($P < 0.01$)
Df(3L)Scf-R6	66E1-6;66F1-6	7.1 ($n = 210$)	Yes ($P < 0.01$)
Df(3L)Rdl-2	66F5;66F5	3.3 ($n = 153$)	No
Df(3L)29A6	66F5;67B1	2.2 ($n = 89$)	No
Df(3L)AC1	67A2;67D11-13	0 ($n = 74$)	No
Df(3L)lxd6	67E1-2;68C1-2	0 ($n = 109$)	No
Df(3L)vin2	67F2-3;68D6	2.7 ($n = 113$)	No
Df(3L)vin5	68A2-3;69A1-3	0 ($n = 92$)	No
Df(3L)vin7	68C8-11;69B4-5	0 ($n = 92$)	No
Df(3L)iro-2	69B1-5;69D1-6	0.8 ($n = 124$)	No
In(3LR)C190	69F3-4;70C3-4 + 89;89	0 ($n = 83$)	No
Df(3L)fz-GF3b	70C2;70D5	1.2 ($n = 85$)	No
Df(3L)fz-M21	70D2-3;71E4-5	2.1 ($n = 94$)	No
Df(3L)BK10	71C;71F	1.2 ($n = 81$)	No
Df(3L)brm11	71F1-4;72D1-10	5.7 ($n = 157$)	Yes ($P < 0.02$)
Df(3L)st-f13	72C1-D1;73A3-4	1.6 ($n = 127$)	No
Df(3L)81k19	73A3;74F	0 ($n = 88$)	No
Df(3L)W10	75A6-7;75C1-2	1.7 ($n = 119$)	No
Df(3L)Cat	75B8;75F1	0 ($n = 127$)	No
Df(3L)VW3	76A3;76B2	5.2 ($n = 134$)	Yes ($P < 0.02$)

(*continued*)

APPENDIX

(Continued)

Deficiency	Cytology	% *enGal4/UASwg* embryos with gaps	Interaction
Df(3L)kto2	76B1-2;76D5	2.4 ($n = 83$)	No
Df(3L)XS-533	76B4;77B	2.3 ($n = 130$)	No
Df(3L)rdgC-co2	77A1;77D1	5.4 ($n = 149$)	Yes ($P < 0.02$)
Df(3L)ri-79c	77B-C;77F-78A	34.2 ($n = 111$)	Yes ($P < 0.001$)
Df(3L)ME107	77F3;78C8-9	0.9 ($n = 107$)	No
Df(3L)Pc-2q	78C5-6;78E3-79A1	2.0 ($n = 153$)	No
Df(3L)Ten-m-AL29	79C1-3;79E3-8	2.9 ($n = 104$)	No
Df(3L)Delta1AK	79F;80A	2.1 ($n = 96$)	No
Df(3R)ME15	81F3-6;82F5-7	1.9 ($n = 104$)	No
Df(3R)6-7	82D3-8;82F3-6	1.2 ($n = 81$)	No
Df(3R)3-4	82F3-4;82F10-11	1.3 ($n = 76$)	No
Df(3R)Tpl10,	83C1-2;84B1-2	0 ($n = 77$)	No
Df(3R)Scr	84A1-2;84B1-2	0 ($n = 78$)	No
Df(3R)p712	84D4-6;85B6	0 ($n = 145$)	No
Df(3R)p-XT103	85A2;85C1-2	0 ($n = 102$)	No
Df(3R)by10	85D8-12;85E7-F1	0.8 ($n = 122$)	No
Df(3R)by62	85D11-14;85F6	0 ($n = 91$)	No
Df(3R)M-Kx1	86C1;87B1-5	0 ($n = 79$)	No
Df(3R)T-32	86E2-4; 87C6-7	1.2 ($n = 82$)	No
Df(3R)ry615	87B11-13;87E8-11	4.1 ($n = 169$)	Yes ($P < 0.05$)
Df(3R)ea	88E7-13;89A1	2.1 ($n = 141$)	No
Df(3R)P115	89B7-8;89E7-8;20	2.8 ($n = 145$)	No
Df(3R)DG2	89E1-F4;91B1-2	1.9 ($n = 104$)	No
Df(3R)Cha7	90F1-4;91F5	2.0 ($n = 98$)	No
Df(3R)Dl-BX12	91F1-2;92D3-6	6.0 ($n = 116$)	Yes ($P < 0.01$)
Df(3R)H-B79	92B3;92F13	2.7 ($n = 113$)	No
Df(3R)e-R1	93B6-7;93D2	2.9 ($n = 103$)	No
Df(3R)e-N19	93B2-13; 94A3-8	1.6 ($n = 127$)	No
Df(3R)mbc-30	95A5-7;95C10-11	2.0 ($n = 101$)	No
Df(3R)mbc-R1	95A5-7;95D6-11	2.5 ($n = 79$)	No
Df(3R)crb-F89-4	95D7-11;95F15	0 ($n = 105$)	No
Df(3R)crb87-5	95F7;96A17-18	1.1 ($n = 88$)	No
Df(3R)Tl-P	97A;98A1-2	0 ($n = 95$)	No
Df(3R)D605	97E3;98A5	0.9 ($n = 115$)	No
Df(3R)3450	98E3;99A6-8	0 ($n = 109$)	No
Df(3R)Dr-rv1	99A1-2;99B6-11	1.4 ($n = 72$)	No
Df(3R)awd-KRB	100D1;100D3-4	36.0 ($n = 136$)	Yes ($P < 0.001$)
Df(3R)faf-BP	100D;100F5	0.9 ($n = 107$)	No
	Secondary screen		
Region 66			
Df(3L)Scf-R11	66E3-4; 66F1-2	1.8 ($n = 172$)	No
dally^{10}	66E1-3	10.1 ($P < 0238$)	Yes ($P < 0.001$)
dally^{E385}	66E1-3	6.3 ($P < 0221$)	Yes ($P < 0.05$)
l(3)06464(dally^{P2}*)*	66E1-2	2.5 ($n = 80$)	No
l(3)01629	66E1-2	1.1 ($n = 347$)	No
Region 72			
Df(3L)A27	70E; 72A3-4	1.0 ($n = 99$)	No
Df(3L)th102	72B1-72D12	18.6 ($n = 156$)	Yes ($P < 0.001$)
brm^{2}	72C1	7.3 ($n = 150$)	Yes ($P < 0.001$)
brm^{T362}	72C1	1.9 ($n = 103$)	No
brm^{T485}	72C1	0 ($n = 139$)	No
arf^{72A}	72C1	2.0 ($n = 108$)	No
Not^{3}	72D1	17.0 ($n = 112$)	Yes ($P < 0.001$)
Not^{5}	72D1	8.3 ($n = 96$)	Yes ($P < 0.001$)
Region 75			
Df(3L)Dfz2	75F10-11;76A1-5	8.0 ($n = 209$)	Yes ($P < 0.001$)

(*continued*)

APPENDIX

(Continued)

Deficiency	Cytology	% *enGal4/UASwg* embryos with gaps	Interaction
Dfz2^{C1}	75F9-10	0 (n = 92)	No
pip^{1}	76A3	0 (n = 99)	No
pip^{2}	76A3	3.2 (n = 124)	No
Region 77			
Df(3L)XS-543	76B; 77A	7.6 (n = 144)	Yes ($P < 0.001$)
psn^{B3}	77B9-C1	1.5 (n = 135)	No
psn^{C4}	77B9-C1	1.0 (n = 111)	No
Region 87			
Df(3R)l26c	87E1; 87F11	9.2 (n = 129)	Yes ($P < 0.001$)
Df(3R)ry75	87D2; 87D14	8.3 (n = 120)	Yes ($P < 0.001$)
Df(3R)urd	87F1-15	8.8 (n = 113)	Yes ($P < 0.001$)
Df(3R)lc4a	87E5-4; E11	1.7 (n = 113)	No
Region 92			
Df(3R)Dl-A143	91F13; 92A2-3	3.3 (n = 151)	No
Dl^{3}	92A1-2	3.3 (n = 123)	No

The cytology of each deficiency and gene is given according to FlyBase (http://flybase.bio.indiana.edu/). The percentage of *enGal4/UASwg* embryos presenting ectopic naked cuticle (gaps) is given for each chromosome tested. A χ^2 was performed for each result, using the number of embryos with gaps found with wild-type chromosomes as the expected frequency (see MATERIALS AND METHODS). A mutant chromosome was considered interacting when the *P*-value was <0.05. Interacting deficiencies or mutants are underlined. *n*, the total number of embryos of genotype *enGal4/UASwg* examined.